HFSZEEMAN95 – A program for computing weak and intermediate magnetic-field- and hyperfine-induced transition rates

Wenxian Li[a,*], Jon Grumer[b], Tomas Brage[c], Per Jönsson[a,*]

[a] *Group for Materials Science and Applied Mathematics, Malmö University, S-20506, Malmö, Sweden*
[b] *Theoretical Astrophysics, Uppsala University, 751-20 Uppsala, Sweden*
[c] *Division of Mathematical Physics, Department of Physics, Lund University, 221-00 Lund, Sweden*

Abstract

HFSZEEMAN95 is an updated and extended Fortran 95 version of the HFSZEEMAN program [Comput. Phys. Commun. 178 (2008) 156-170]. Given relativistic atomic state functions generated by the GRASP2018 package [Comput. Phys. Commun. 237 (2019) 184187], HFSZEEMAN95 together with the accompanying Matlab/GNU Octave program MITHIT allows for: (1) the computation and plotting of Zeeman energy splittings of magnetic fine- and hyperfine structure substates as functions of the strength of an external magnetic field, (2) the computation of transition rates between different magnetic fine- and hyperfine structure substates in the presence of an external magnetic field and rates of hyperfine-induced transitions in the field free limit, (3) the synthesization of spectral profiles for transitions obtained from (2). With the new features, HFSZEEMAN95 and the accompanying Matlab/GNU Octave program MITHIT are useful for the analysis of observational spectra and to resolve the complex features due to the splitting of the fine and hyperfine levels.

Keywords: Relativistic atomic wave functions; Hyperfine structure; Zeeman effect; Magnetic field; Multiconfiguration Dirac-Hartree-Fock+Breit; Unexpected transitions; Hyperfine-induced

*Corresponding author.
E-mail address: wenxianli10@yahoo.com, per.jonsson@mau.se

transitions; Magnetic-field-induced transitions

PROGRAM SUMMARY

Program Title: HFSZEEMAN95
Licensing provisions: GNU General Public License 3 (GPL)
Programming language: Fortran 95, Matlab/GNU Octave
Nature of problem: Calculation of transition energies and rates between different magnetic fine- and hyperfine structure substates in the presence of an external magnetic field and rates of hyperfine induced transitions in the field free limit. Synthesization of spectral profiles.
Solution method: Wave functions for magnetic fine structure substates in the field free case are given by atomic state functions (ASFs). The ASFs are expansions over configuration state functions (CSFs)

$$|\Gamma J M_J\rangle = \sum_\gamma c_\gamma |\gamma J M_J\rangle.$$

The ASFs are computed by the GRASP2018 relativistic atomic structure package [17] and are supposed to be available. Wave functions for magnetic fine structure substates in an external magnetic field are expanded in a basis of ASFs

$$|\widetilde{\Gamma} M_J\rangle = \sum_{\Gamma J} d_{\Gamma J} |\Gamma J M_J\rangle.$$

Wave functions for magnetic hyperfine structure substates in an external magnetic field are expanded in a basis of the combined nuclear and atomic system

$$|\widetilde{\Gamma} I M_F\rangle = \sum_{\Gamma J F} d_{\Gamma J F} |\Gamma I J F M_F\rangle,$$

where $|\Gamma I J F M_F\rangle$ are coupled nuclear and atomic functions

$$|\Gamma I J F M_F\rangle = \sum_{M_I, M_J} \langle I J M_I M_J | I J F M_F\rangle |I M_I\rangle |\Gamma J M_J\rangle.$$

Reduced hyperfine and Zeeman matrix elements, used to construct the total interaction matrix in the given basis, are computed as sums over reduced one-particle matrix elements of orbitals building the CSFs. By diagonalizing the interaction matrix, Zeeman energy splittings of fine- and hyperfine structure substates are obtained together with the expansion coefficients of the basis functions. Transition rates between different magnetic fine- and hyperfine structure substates are computed as sums over reduced transition matrix elements between fine structure

states weighted by the expansion coefficients of the basis functions and angular factors. Given energies of the magnetic substates along with transition rates, a synthetic spectrum is obtained by convolving the spectral lines with a Gaussian function with a user defined value of the full width half maximum (FWHM).
Additional comments including Restrictions and Unusual features : 1. The complexity of the cases that can be handled is determined by the GRASP2018 package used for the generation of the atomic state functions. 2. The current programs can be used for the calculations of electric dipole (E1), electric quadrupole (E2), magnetic dipole (M1) and magnetic quadrupole (M2) magnetic-field- and hyperfine-induced transitions, which are caused by the mixing of states due to hyperfine and Zeeman interaction. 3. The present model does not include the necessary non-perturbative treatment of the uncommon case involving near-degeneracies where the radiative width of a fine structure state is of the same order as the hyperfine or magnetic-field perturbation; an effect often termed radiation damping [1, 2, 3].

1. Introduction

Hyperfine-induced (HIT) and magnetic-field-induced (MIT) transitions have been theoretically and experimentally studied for various atomic systems due to their potential applications in plasma diagnostics, e.g. the determination of electron densities, isotope compositions, and magnetic fields [4, 5, 6, 7, 8, 9]. The development of programs for computing rates of the corresponding transitions along with synthetic spectra is essential for utilizing their diagnostic potential. The programs have direct applications for the analysis of spectra from e.g. electron-beam ion trap (EBIT) sources as well as of stellar spectra, especially from magnetic stars. As an example of the latter, it has been illustrated for the Li I doublet lines @ 6708 Å in cool magnetic Ap stars that there can be significant departures from the linear Zeeman splitting pattern, due to the mixing of states caused by the external magnetic field [10].

There are a number of atomic structure packages such as the Atomic Structure Package [11, 12], the Flexible Atomic Code [13], the Jena Atomic Calculator [14], the CI-MBPT package [15] and the General Relativistic Atomic Structure Package [16]. The latter, with GRASP2018 as the latest version [17], is based on the fully relativistic multiconfiguration Dirac-Hartree-Fock (MCDHF) method [18]. The package consists of a number of application programs and tools to compute approximate relativistic wave functions, energy levels, transition rates and a number of other properties, see e.g. [19, 20]. HFSZEEMAN is the application program used to compute reduced electronic hyperfine and Zeeman matrix elements as well as Landé g_J factors and, if the nuclear spin I is non-zero, magnetic dipole A_J and electric quadrupole B_J hyperfine interaction constants [21]. The accompany-

ing Matlab/GNU Octave program PLOTHFSZEEMAN computes the Zeeman energy splittings of fine- and hyperfine structure substates in an external magnetic field and the expansion coefficients of these substates in a basis of atomic state functions [21]. We have translated HFSZEEMAN Fortran 77 to Fortran 95 and adapted it to GRASP2018. In addition we have developed a Matlab/GNU Octave program MITHIT with PLOTHFSZEEMAN, TRANS, and GAUSSPLOT as the main subroutines. MITHIT contains all the functionality of the original PLOTHFSZEEMAN program. In addition MITHIT allows for the calculation of transition rates between magnetic substates/hyperfine levels and the construction of synthetic spectra. The operation of the new programs are illustrated in a number of examples.

2. Theory

2.1. Wave functions for fine structure states

In the MCDHF method [22] the electronic wave functions, frequently referred to as the atomic state functions (ASFs), for fine structure states are expanded in antisymmetrized and jj-coupled configuration state functions (CSFs), which are eigenfunctions of $\mathbf{J}^2, J_z$ and parity

$$|\Gamma J M_J\rangle = \sum_\gamma c_\gamma |\gamma J M_J\rangle. \tag{1}$$

The CSFs are sums of products of four-component spin-orbitals

$$\langle \mathbf{r} | n\kappa m\rangle = \frac{1}{r} \begin{pmatrix} P_{n\kappa}(r)\chi_{\kappa m}(\widehat{r}) \\ \mathrm{i}Q_{n\kappa}(r)\chi_{-\kappa m}(\widehat{r}) \end{pmatrix}, \tag{2}$$

where n is the principal quantum number and κ is the relativistic angular quantum number. $P_{n\kappa}(r)$ and $Q_{n\kappa}(r)$ are the large and small component radial wave functions and $\chi_{\kappa m}(\widehat{\mathbf{r}})$ are the spinor spherical harmonics in the lsj-coupling scheme. The radial functions $P_{n\kappa}(r)$ and $Q_{n\kappa}(r)$ are represented on a logarithmic grid and are required to be orthonormal within each κ symmetry. The radial functions and the expansion coefficients for the CSFs are obtained by iteratively solving the equations resulting from applying the variational principle on an averaged energy functional based on the fine structure Hamiltonian H_{fs} with additional terms needed to preserve the orthonormality of the radial orbitals within each κ symmetry. The computation of the ASFs are done with the GRASP2018 program package [17].

2.2. Hyperfine structure

The hyperfine structure of an atomic energy level is caused by the non-central interaction between the electrons and the electromagnetic multipole moments of the nucleus. The Hamiltonian for the interaction is given by a multipole expansion

$$H_{hfs} = \sum_{k\geq 1} \mathbf{T}^{(k)} \cdot \mathbf{M}^{(k)}, \tag{3}$$

where $\mathbf{T}^{(k)}$ and $\mathbf{M}^{(k)}$ are spherical tensor operators of rank k in the electronic and nuclear spaces, respectively [23]. For an N-electron atom the electronic tensor operators for the leading contributions, the magnetic dipole and the electric quadrupole, are

$$\mathbf{T}^{(1)} = \sum_{j=1}^{N} \mathbf{t}^{(1)}(j) = \sum_{j=1}^{N} -\mathrm{i}\sqrt{2}\alpha\, r_j^{-2} \left(\boldsymbol{\alpha}_j\, \mathbf{C}^{(1)}(j)\right)^{(1)} \tag{4}$$

$$\mathbf{T}^{(2)} = \sum_{j=1}^{N} \mathbf{t}^{(2)}(j) = \sum_{j=1}^{N} -r_j^{-3}\mathbf{C}^{(2)}(j). \tag{5}$$

In the formulas above α is the fine structure constant, $\boldsymbol{\alpha}$ is the Dirac matrix and $\mathbf{C}^{(k)}$ is a spherical tensor operator of rank k.

Adding the hyperfine interaction to the relativistic fine structure Hamiltonian we obtain

$$H = H_{fs} + H_{hfs}. \tag{6}$$

The hyperfine interaction couples the nuclear $\mathbf{I}$ and electronic $\mathbf{J}$ angular momenta to a total momentum $\mathbf{F} = \mathbf{I} + \mathbf{J}$, and we represent the wave functions of the hyperfine states by expansions

$$|\widetilde{\Gamma} F M_F\rangle = \sum_{\Gamma J} d_{\Gamma J} |\Gamma I J F M_F\rangle, \tag{7}$$

where $|\Gamma I J F M_F\rangle$ are coupled nuclear and electronic wave functions

$$|\Gamma I J F M_F\rangle = \sum_{M_I, M_J} \langle I J M_I M_J | I J F M_F\rangle |I M_I\rangle |\Gamma J M_J\rangle. \tag{8}$$

This representation of the wave functions leads to the matrix eigenvalue problem

$$\mathsf{Hd} = E\mathbf{d}, \tag{9}$$

where H is the matrix with elements

$$H_{\Gamma J, \Gamma' J'} = \langle \Gamma I J F M_F | H_{fs} + \mathbf{T}^{(1)} \cdot \mathbf{M}^{(1)} + \mathbf{T}^{(2)} \cdot \mathbf{M}^{(2)} | \Gamma' I J' F M_F\rangle. \tag{10}$$

The matrix elements of the fine structure Hamiltonian H_{fs} are diagonal in all quantum numbers and equal the calculated fine structure energies $E_{\Gamma J}$. The hyperfine interaction matrix elements can be expressed in terms of reduced electronic and nuclear matrix elements, and explicit formulas are given in the write-up of HFSZEEMAN [21]. The electronic matrix elements are computed as sums over radial one-electron matrix elements weighted by angular coefficients, see [21], section 2.5. The nuclear matrix elements are given in terms of the experimentally determined nuclear magnetic dipole moment μ_I and electric quadrupole moment Q, see [24] for a recent tabulation.

2.3. Zeeman effect of fine structure substates

Neglecting diamagnetic contributions and choosing the direction of the external magnetic field $\mathbf{B}$ as the z-direction, the interaction between the atomic electrons and the field can be written

$$H_m = (\mathbf{N}^{(1)} + \Delta\mathbf{N}^{(1)}) \cdot \mathbf{B} \equiv (N_0^{(1)} + \Delta N_0^{(1)})B, \tag{11}$$

where $B = |\mathbf{B}|$ is the strength of the magnetic field. The last term is the so called Schwinger QED correction. For an N-electron atom the electronic tensor operators are [25], in atomic units,

$$\mathbf{N}^{(1)} = \sum_{j=1}^{N} \mathbf{n}^{(1)}(j) = \sum_{j=1}^{N} -\mathrm{i}\frac{\sqrt{2}}{2\alpha}\, r_j \left(\boldsymbol{\alpha}_j\, \mathbf{C}^{(1)}(j)\right)^{(1)}, \tag{12}$$

$$\Delta\mathbf{N}^{(1)} = \sum_{j=1}^{N} \Delta\mathbf{n}^{(1)}(j) = \sum_{j=1}^{N} \frac{g_s - 2}{2}\beta_j \boldsymbol{\Sigma}_j, \tag{13}$$

where $\boldsymbol{\Sigma}_j$ is the relativistic spin-matrix and $g_s = 2.00232$ the g factor of the electron spin corrected for QED effects.

In the intermediate field regime we consider the total Hamiltonian

$$H = H_{fs} + H_m. \tag{14}$$

When the field is included only M_J remains a good quantum number, and the wave function can be written as an expansion

$$|\widetilde{\Gamma} M_J\rangle = \sum_{\Gamma J} d_{\Gamma J} |\Gamma J M_J\rangle. \tag{15}$$

Just as for the hyperfine interaction this leads to a matrix eigenvalue problem

$$\mathsf{H}\mathbf{d} = E\mathbf{d}, \tag{16}$$

where $\mathbf{H}$ is the matrix with elements

$$H_{\Gamma J,\Gamma' J'} = \langle \Gamma J M_J | H_{fs} + (\mathbf{N}^{(1)} + \Delta\mathbf{N}^{(1)}) \cdot \mathbf{B} | \Gamma' J' M_J \rangle. \tag{17}$$

The matrix elements of the fine structure Hamiltonian H_{fs} are diagonal in all quantum numbers and equals the energies $E_{\Gamma J}$ of the fine structure levels. The Zeeman interaction matrix elements can be expressed in terms of the reduced electronic matrix elements and the strength of the magnetic field. Explicit formulas are given in [21]. Again, the electronic matrix elements are computed a sums over radial one-electron matrix elements weighted by angular coefficients. By diagonalizing the interaction matrix and plotting eigenvalues as functions of the strength B of the magnetic field, Zeeman energy splittings of the magnetic fine structure substates are obtained.

2.4. Zeeman effect of hyperfine structure substates

We now describe the Zeeman effect of hyperfine structure substates. If we choose the direction of the magnetic field as the z-direction the interaction can be written

$$\begin{aligned} H_m &= (\mathbf{N}^{(1)} + \Delta\mathbf{N}^{(1)}) \cdot \mathbf{B} + \text{interaction with nucleus} \\ &\equiv (N_0^{(1)} + \Delta N_0^{(1)}) B + \text{interaction with nucleus.} \end{aligned} \tag{18}$$

The interaction of the magnetic field with the nucleus is small and can, just as the diamagnetic contributions, be neglected [26, 27].

The total Hamiltonian is now given by

$$H = H_{fs} + H_{hfs} + H_m. \tag{19}$$

In this case M_F is the only good quantum number, and we represent the wave function by the expansion

$$|\widetilde{\Gamma} I M_F\rangle = \sum_{\Gamma J F} d_{\Gamma J F} |\Gamma I J F M_F\rangle. \tag{20}$$

This leads to the matrix eigenvalue problem

$$\mathbf{H}\mathbf{d} = E\mathbf{d}, \tag{21}$$

where $\mathbf{H}$ is the matrix with elements

$$\begin{aligned} H_{\Gamma J F,\Gamma' J' F'} = \langle \Gamma I J F M_F | H_{fs} + \mathbf{T}^{(1)} \cdot \mathbf{M}^{(1)} \\ + \mathbf{T}^{(2)} \cdot \mathbf{M}^{(2)} + (\mathbf{N}^{(1)} + \Delta\mathbf{N}^{(1)}) \cdot \mathbf{B} | \Gamma' I J' F' M_F \rangle. \end{aligned} \tag{22}$$

Formulas for the relevant matrix elements are given in [21]. All electronic matrix elements are computed as sums over radial one-electron matrix elements weighted by angular coefficients.

2.5. Transition rates between magnetic fine structure substates

The transition rate in s^{-1} for an electric dipole (E1) transition between an upper $\widetilde{\Gamma}'M'_J$ and a lower $\widetilde{\Gamma}M_J$ magnetic fine structure substate is given by

$$A(\widetilde{\Gamma}'M'_J \to \widetilde{\Gamma}M_J) = \frac{2.02613\times 10^{18}}{\lambda^3}\sum_q |\langle \widetilde{\Gamma}M_J|P_q^{(1)}|\widetilde{\Gamma}'M'_J\rangle|^2, \tag{23}$$

where $P_q^{(1)}$ is the electric dipole operator in the length gauge in atomic units. λ is the wavelength in Ångström. Substituting Eq. (15) into Eq. (23) and using the Wigner-Eckart theorem, the rate can be rewritten as

$$A(\widetilde{\Gamma}'M'_J \to \widetilde{\Gamma}M_J) =$$
$$= \frac{2.02613\times 10^{18}}{\lambda^3}\sum_q \left| \sum_{\Gamma J}\sum_{\Gamma' J'} d_{\Gamma J} d'_{\Gamma' J'} (-1)^{J-M_J} \begin{pmatrix} J & 1 & J' \\ -M_J & q & M'_J \end{pmatrix} \langle \Gamma J||\mathbf{P}^{(1)}||\Gamma' J'\rangle \right|^2, \tag{24}$$

where the reduced transition matrix element is the square root of the line strength $S_{\Gamma J\Gamma' J'}$ multiplied with a phase factor

$$\langle \Gamma J\|\mathbf{P}^{(1)}\|\Gamma' J'\rangle = \text{phase factor} \times S^{1/2}_{\Gamma J\Gamma' J'}. \tag{25}$$

The reduced matrix elements in Eq. (24), including the phase factors, are computed by a modified version of the transition program belonging to the GRASP2018 package [17]. The modified version, RTRANSITION_PHASE and the MPI version RTRANSITION_PHASE_MPI, is provided in the present program submission.

2.6. Transition rates between magnetic hyperfine structure substates

The transition rate for an electric dipole transition between an $\widetilde{\Gamma}'M'_F$ and a lower $\widetilde{\Gamma}M_F$ magnetic hyperfine structure substate is given by

$$A(\widetilde{\Gamma}'M'_F \to \widetilde{\Gamma}M_F) = \frac{2.02613\times 10^{18}}{\lambda^3}\sum_q |\langle \widetilde{\Gamma}M_F|P_q^{(1)}|\widetilde{\Gamma}'M'_F\rangle|^2. \tag{26}$$

Substituting Eq. (20) into Eq. (26) and using the Wigner-Eckart theorem together with an uncoupling of F, the rate can be rewritten as

$$A(\widetilde{\Gamma}'M'_F \to \widetilde{\Gamma}M_F) = \frac{2.02613\times 10^{18}}{\lambda^3}\sum_q \left| \sum_{\Gamma JF}\sum_{\Gamma' J'F'} d_{\Gamma JF} d'_{\Gamma' J'F'} \right.$$
$$\times \sqrt{(2F'+1)(2F+1)}(-1)^{F-M_F} \begin{pmatrix} F & 1 & F' \\ -M_F & q & M'_F \end{pmatrix} (-1)^{I+J'+F+1} \tag{27}$$
$$\left. \begin{Bmatrix} J & F & I \\ F' & J' & 1 \end{Bmatrix} \langle \Gamma J||\mathbf{P}^{(1)}||\Gamma' J'\rangle \right|^2.$$

Again the reduced transition matrix element is the square root of the line strength $S_{\Gamma J\Gamma' J'}$ multiplied with a phase factor.

2.7. Transition rates between hyperfine structure levels

Setting $B = 0$, with F and M_F as good quantum numbers, the total transition rate from a substate $\widetilde{\Gamma}'F'M'_F$ to all M_F substates of the level $\widetilde{\Gamma}F$ is given by

$$A(\widetilde{\Gamma}'F'M'_F \to \widetilde{\Gamma}F) = \frac{2.02613 \times 10^{18}}{\lambda^3} \sum_{q,M_F} |\langle \widetilde{\Gamma}FM_F|P_q^{(1)}|\widetilde{\Gamma}'F'M'_F\rangle|^2. \tag{28}$$

Inserting Eq. (7) into the expression above, using the Wigner-Eckart theorem and the summation properties of the 3-j symbols together with an uncoupling of F, we obtain

$$\begin{aligned} A(\widetilde{\Gamma}'F'M'_F \to \widetilde{\Gamma}F) = \frac{2.02613 \times 10^{18}}{\lambda^3}(2F+1)\Bigg| \sum_{\Gamma J} \sum_{\Gamma' J'} d_{\Gamma J} d'_{\Gamma' J'} \\ \times (-1)^{I+J'+F+1} \begin{Bmatrix} J & F & I \\ F' & J' & 1 \end{Bmatrix} \langle \Gamma J||\mathbf{P}^{(1)}||\Gamma' J'\rangle \Bigg|^2. \end{aligned} \tag{29}$$

The transition rate above is independent of M'_F, and this quantum number is often left out in the notation.

2.8. Higher transition moments

The program is also applied for the computation of the rates of electric quadrupole (E2), magnetic dipole (M1) and magnetic quadrupole (M2) magnetic-field- and hyperfine-induced transitions of which the theory is not present here. The detailed theory for higher transition moments can be found in [26].

3. Program Structure

The present package consists of a Fortran 95 program HFSZEEMAN95 and a Matlab/GNU Octave[1] program MITHIT. There is also a modified transition program, RTRANSITION_PHASE/RTRANSITION_PHASE_MPI, belonging to GRASP2018 that, in addition to the weighted oscillator strengths, transition rates and line strengths, computes the reduced transition matrix element in Eq. (25).

3.1. HFSZEEMAN95*: the translation from F77 to F95*

Given ASFs generated by the GRASP2018 package, HFSZEEMAN95 computes Landé g_J factors and, if the nuclear spin I is non-zero, also magnetic dipole A_J and electric quadrupole B_J hyperfine interaction constants. In addition the program

[1]Matlab is a registered trademark of The MathWorks, Inc.

computes reduced electronic hyperfine and Zeeman matrix elements used to construct the total interaction matrix. HFSZEEMAN95 is a translation of HFSZEEMAN [21] from Fortran 77 standard to free-format Fortran 95 (F95) standard without changing the basic structure of the program. In the new version, MODULEs are used instead of COMMON blocks. The IMPLICIT NONE statement is used so that all variables of a routine is defined explicitly and interfaces were created for calling procedures. The non-standard Cray Pointer were replaced by standard F95 pointers. HFSZEEMAN95 is an integrated part of GRASP2018.

3.2. MITHIT

Given the output files of HFSZEEMAN95 and the modified transition program RTRANSITION_PHASE/RTRANSITION_PHASE_MPI, the Matlab/GNU Octave program MITHIT computes and outputs energies of the magnetic substates, expansion coefficients for the basis functions and transition rates between different magnetic fine- (MIT-fs) and hyperfine (MIT-hfs) structure substates in an external magnetic field. In the field free limit MITHIT computes and outputs rates of hyperfine induced transitions (HIT). Based on the computed transition rates MITHIT can be used to generate synthetic spectra through a convolution with a Gaussian function with a given full width half maximum (FWHM). The main subroutines in MITHIT are PLOTHFSZEEMAN, TRANS and GAUSSPLOT.

3.2.1. PLOTHFSZEEMAN

PLOTHFSZEEMAN originates from [21] and is kept as a separate subroutine of MITHIT. In response to user input (MIT-fs, HIT or MIT-hfs) the subroutine reads nuclear parameters from the terminal (automatically sets $I = 0$ with the HIT selection). Given the nuclear parameters and the list of ASFs defined in the output file of HFSZEEMAN95, the subroutine determines the structure of the basis functions. For $I \neq 0$ the basis functions are

$$|\Gamma I J F M_F\rangle = \sum_{M_I, M_J} \langle I J M_I M_J | I J F M_F\rangle |I M_I\rangle |\Gamma J M_J\rangle \tag{30}$$

with $|I-J| \leq F \leq I+J$. For $I = 0$ the basis functions are $|\Gamma J M_J\rangle$. The subroutine subsequently reads the hyperfine and magnetic reduced matrix elements from the HFSZEEMAN95 output file, constructs and diagonalizes the interaction matrix for different values of B and plots the energies of the magnetic substates as functions of B. For the largest specified value of the magnetic field, the energies of the magnetic substates and the expansion coefficients of the basis functions are written to file and saved for the calculation of transition rates. Few errors in PLOTHFSZEEMAN of [21] has been corrected in the present version.

3.2.2. TRANS

The TRANS subroutine computes all rates in a transition array. TRANS reads the mixing coefficients for the basis functions as determined by PLOTHFSZEEMAN along with the reduced transition matrix elements $\langle \Gamma J || \mathbf{P}^{(1)} || \Gamma' J' \rangle$ computed by RTRANSITION_PHASE/RTRANSITION_PHASE_MPI. The subroutine goes on to determine the needed 3-j and 6-j symbols and sums up, depending on the case, all the contributions according to Eqs. (24, 27, 29) to yield the transition rates $A(\widetilde{\Gamma}' M'_J \rightarrow \widetilde{\Gamma} M_J)$, $A(\widetilde{\Gamma}' M'_F \rightarrow \widetilde{\Gamma} M_F)$, and $A(\widetilde{\Gamma}' F' M'_F \rightarrow \widetilde{\Gamma} F)$, respectively. The rates are written to file.

3.2.3. GAUSSPLOT

The GAUSSPLOT subroutine reads the transition arrays computed by TRANS and generates a synthetic spectrum. Each magnetic/hyperfine component is convoluted with a Gaussian function with given FWHM.

4. Input and Output Data

The input and output for the different programs involved in the computation are schematically shown in Fig. 1.

4.1. HFSZEEMAN95

This program adheres to the GRASP2018 naming conventions, and the $\langle name \rangle$ of the files defining the ASFs has to be specified. The program reads data from the configuration list file $\langle name \rangle$.c, the radial wave function file $\langle name \rangle$.w and, dependent on whether the atomic state functions originate from an MCDHF or RCI calculation, from the mixing file $\langle name \rangle$.m or $\langle name \rangle$.cm. Values of the nuclear spin, magnetic dipole and quadrupole moments are read from the file *isodata*. The program produces two output files $\langle name \rangle$.(c)gjhfs and $\langle name \rangle$.(c)h, where the letter c in the extension indicates that the input data are from an RCI calculation. In the file $\langle name \rangle$.(c)gjhfs the program outputs the J quantum numbers and energies $E_{\Gamma J}$ of the atomic states together with the reduced hyperfine and Zeeman matrix elements. In the file $\langle name \rangle$.(c)h the program outputs the energies and the diagonal Landé g_J factors, and if the isotope has a nuclear spin, the diagonal A_J and B_J hyperfine constants.

4.2. RTRANSITION_PHASE/RTRANSITION_PHASE_MPI

Given $\langle name1 \rangle$ and $\langle name2 \rangle$ of the lower and upper ASFs, the modified transition program RTRANSITION_PHASE opens and reads the data from the configuration list files $\langle name1 \rangle$.c and $\langle name2 \rangle$.c, the biorthogonally transformed radial wave function files $\langle name1 \rangle$.bw and $\langle name2 \rangle$.bw, and dependent on whether

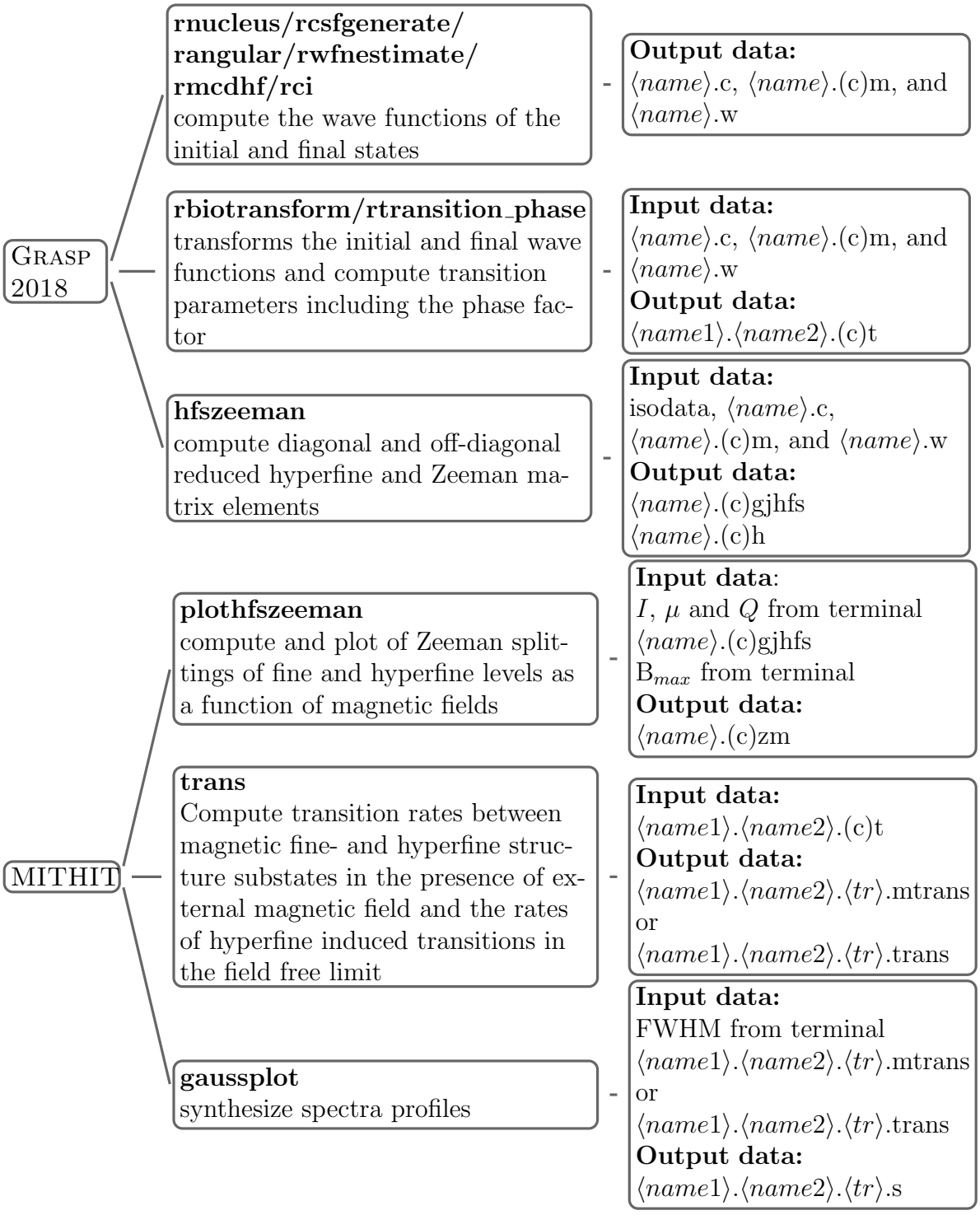

Figure 1: Program operation and data flow of program involved in the computation. $\langle name1\rangle$ and $\langle name2\rangle$ are the names of the initial and final states. $\langle tr\rangle$ is the type of the transitions which are hfs.mit, fs.mit and hfs.hit corresponds to the three types of transitions MIT-hfs, MIT-fs and HIT, respectively.

the atomic state functions originate from an MCDHF or RCI calculation, from the transformed mixing files ⟨*name*1⟩.bm and ⟨*name*2⟩.bm or ⟨*name*1⟩.cbm and ⟨*name*2⟩.cbm. The program outputs the file ⟨*name*1⟩.⟨*name*1⟩.(c)t containing weighted oscillator strengths, rates, line strengths and phase factors (Eq. (25)) for all transitions.

4.3. MITHIT

Given the ⟨*name*1⟩ and ⟨*name*2⟩ of the lower and upper ASFs, MITHIT opens and reads ⟨*name*1⟩.(c)gjhfs and ⟨*name*2⟩.(c)gjhfs. The program asks for the transition type. As an example, if MIT-hfs is chosen, the program reads the nuclear parameters, namely nuclear spin I , the nuclear magnetic dipole moment μ_I , the nuclear electric quadrupole moment Q from the terminal. The maximum magnetic field should be given, in Tesla or Gauss, and the units of energy should be chosen to a.u., cm^{-1} or MHz. The computations are performed by HFSZEEMAN as described in the previous section. The user has the possibility to plot energies of the magnetic substates as functions of the strength of the magnetic field. After the plotting, the field free energies on the hyperfine structure levels are printed to the files ⟨*name*1⟩.(c)zm and ⟨*name*2⟩.(c)zm, together with the energies and expansion coefficients of the basis functions for the magnetic substates at the largest specified value of the magnetic field. The program asks whether to continue to the TRANS subroutine. If the answer is "no" the MITHIT halts. Otherwise the program goes on and opens and reads the file ⟨*name*1⟩.⟨*name*1⟩.(c)t and asks for the index of the lower and upper levels of the target transitions. If MIT-hfs is chosen, the TRANS subroutine computes and outputs the transition rates $A(\widetilde{\Gamma}' M'_F \rightarrow \widetilde{\Gamma} M_F)$ between magnetic hyperfine substates together with the transition energies to the file ⟨*name*1⟩.⟨*name*2⟩.hfs.mit.mtrans. If MIT-fs is chosen TRANS computes and outputs the transition rates $A(\widetilde{\Gamma}' M'_J \rightarrow \widetilde{\Gamma} M_J)$ together with the transition energies to the file ⟨*name*1⟩.⟨*name*2⟩.fs.mit.mtrans. If HIT is chosen TRANS computes and outputs the transition rates between the hyperfine structure states $A(\widetilde{\Gamma}' F' M'_F \rightarrow \widetilde{\Gamma} F)$ to the file ⟨*name*1⟩.⟨*name*2⟩.hfs.hit.trans. Finally, the program asks whether to continue to the GAUSSPLOT subroutine for a plot of synthetic spectra. If the answer is "no" the MITHIT halts. Otherwise the program goes on and asks for the index of the lower and upper levels of the target spectral lines. By reading the energies of the magnetic substates along with transition rates from file ⟨*name*1⟩.⟨*name*2⟩.⟨*tr*⟩.mtrans or ⟨*name*1⟩.⟨*name*2⟩.⟨*tr*⟩.trans, a synthetic spectrum is obtained by convolving the spectral lines with a Gaussian function with a user defined value of the FWHM and the spectra data are written to the file ⟨*name*1⟩.⟨*name*2⟩.⟨*tr*⟩.s.

The calculations in MITHIT are normally done in default double precision arithmetic. In some case it may, however, be necessary to switch to variable precision

arithmetic which evaluates each element of the symbolic input to defined significant digits.

5. Installation

Installation of the programs assumes that the GRASP2018 package [17] is available and properly installed. Start the installation procedure by copying the `hfszeeman95.tar.gz` file to the `grasproot/src/appl` directory, where `grasproot` is the root directory of your current installation of GRASP2018. Uncompress the tar file and give the unix `tar -xvf` command. This will build the directory `hfszeeman95` with the subdirectories `examples`, `hfszeeman95`, `mithit`, `rtransition_phase` and `rtransition_phase_mpi`. To compile the HFSZEEMAN95 source code go to the `hfszeeman95` directory and set the environment variables in `Makefile`. Specifically, make sure that the GRASP2018 root directory corresponds to that of your current installation, see the installation procedure as described in [17]. Once the environment variables are set issue the `make` command. If the compilation and linking is successful, the executable will automatically be transferred to the `grasproot/bin` directory. To compile the RTRANSITION_PHASE source code go to the `rtransition_phase/rtransition_phase_mpi` subdirectory and follow the steps above. Again, the executable will automatically be transferred to the `grasproot/bin` directory.

The Matlab/GNU Octave source code is in the subdirectory `mithit`. The scripts and data files needed to run the six test cases appear in the subdirectories `examples/test1` to `examples/test6`.

Changing to the test directories, test runs described later in the article can now be executed to make sure that the programs works correctly. Matlab/GNU Octave is a interpreting language and there is no need for compilation for this part. Start Matlab/GNU Octave and add the `hfszeeman95/mithit` directory to the path. Change to the test directories and execute the test runs.

6. Test Runs

The programs have been extensively tested. Here we present six test runs to illustrate specific program operations. Test 1, computing and plotting the Zeeman splittings of magnetic hyperfine structure substates of $1s2p\ ^{1,3}P$ in ^{3}He. Test 2, computing and plotting the Zeeman splittings of magnetic fine structure substates of $1s4f\ ^{1,3}F$ and $1s5f\ ^{1,3}F$ in ^{4}He. Test 3, computing and plotting the Zeeman splittings of magnetic fine structure substates of $1s^{2}4d\ ^{2}D$ in ^{6}Li. Test 4, computing hyperfine-induced-transitions in the He-like iso-electronic sequence ($6 \leq Z \leq 30$). Test 5, computing magnetic-field-induced transitions for the

Be-like iso-electronic sequence. Test 6, generation of synthetic spectra for the hyperfine $4s4d\ ^3D_2 - 4s4f\ ^3F_{2,3}$ transition array in Ga II. Preparatory calculations using the programs of GRASP2018 have to be done in order to perform the test runs, and the corresponding scripts are located in `hfszeeman95/test1/script` to `hfszeeman95/test6/script`.

6.1. Test case 1

The first test case is for the Zeeman energy splittings of hyperfine structure substates of $1s2p\ ^3P_{0,1,2}$ in neutral ^{3}He with a nuclear spin of $I = 1/2$ and a nuclear dipole moment of $\mu_I = -2.12749772$ nm. The output file `1s2p.cgjhfs` from HFSZEEMAN95 is obtained by running the GRASP2018 scripts in `examples/test1/script` subdirectory and the fine structure energies are rescaled to the NIST data [28].

The session log for program MITHIT is displayed in Fig. 2. The plot of the energies of the magnetic hyperfine substates of $1s2p\ ^3P_{0,1,2}$ as functions of the strength of the magnetic field up to 10000 G are shown in Fig. 3. In Table 1 we compare the level crossings values with the result of Wu and Drake [29] and available experimental values [30, 31]. It is clear that there is a very good agreement between the results except few values showing somewhat larger differences, e.g. No. 21. The explanation might be the adoption of the double basis set Hylleraas-type variational wave functions [32] in [29], which gives very accurate representations of both correlation and the interaction matrix elements for few-electron atoms.

6.2. Test case 2

The second case is for the Zeeman splitting of fine structure states of $1s4f$ and $1s5f$ in ^{4}He. We run the GRASP2018 scripts in the `examples/test2/script` subdirectory and compute the Zeeman interaction matrix. The produced output file is named `HeI_1snf.cgjhfs`. The fine structure energies are rescaled based on the NIST values [28].

A plot of the energies of the magnetic substates of $1s4f\ ^3F_{2,4}$ ($M_J = \pm 1$ and ± 2) and $1s5f\ ^3F_{2,4}$ ($M_J = \pm 1$ and ± 2) as a function of the strength of the magnetic field (see Fig. 4) is compared with the same plot by Anisimova et al. [33]. Anticrossings are found at 149.15 G and 233.23 G for $1s4f$, and at 72.07 G and 91.59 G for $1s5f$, which correspond to 148 G, 222 G, 73 G and 94 G respectively given in [33].

6.3. Test case 3

The third test case is for the fine structure of $1s^24d\ ^2D_{5/2,3/2}$ for ^{6}Li. GRASP2018 scripts and session log for this test run are located in `examples/test3`.

The magnetic substates are plotted as a function of magnetic field up to 460 G. The five crossing points of the substates are labeled in Fig. 5. The crossing points

are compared with the experimental results [34] in Table 2 and good agreement is found. Please note that the fine structure energies are rescaled to the NIST values [28].

6.4. Test case 4

The hyperfine-induced transition rates $A(1s2p\ ^3P_0\ F' = I\ \rightarrow\ 1s^2\ ^1S_0\ F = I)$ are calculated for He-like ions ($6\ \leq\ Z\ \leq\ 30$). In Table 3 the rates are compared with other theoretical results [35]. Good agreement is found.

Taking He-like ^{19}F as an example, the session log for program MITHIT is shown in Fig. 6 and the corresponding output file `even.odd.hfs.hit.trans` containing the hyperfine structure energies and hyperfine-induced transition rates, as well as the wavelengths are displayed in Fig. 7. The hyperfine structure energies are in unit of a.u. and the wavelengths are given in cm^{-1} (Kays).

6.5. Test case 5

Magnetic-field-induced transitions have been studied in various atomic systems, e.g. Be-like ions [36, 37], Ne-like ions [38, 37] and Cl-like ions [8, 9].

Here we present the calculations for the transition rates $A(2s2p\ ^3P_0\ M'_F \rightarrow\ 2s^2\ ^1S_0\ M_F)$ and $A(2s2p\ ^3P_0\ M'_J \rightarrow\ 2s^2\ ^1S_0\ M_J)$ in the presence of an external magnetic field for the isotopes Be-like ^{47}Ti and ^{48}Ti, respectively. ^{47}Ti has a nuclear spin $I = 5/2$, nuclear dipole moment $\mu_I = -0.78848$ nm and nuclear electric quadrupole moment $Q = 0.302$ barn, while ^{48}Ti has $I = \mu_I = Q = 0$.

The session logs for the program MITHIT are displayed in Fig. 8 and 9 for ^{48}Ti and ^{47}Ti, respectively. For ^{48}Ti MITHIT produces the output transition file, `even.odd.fs.mit.mtrans` (see Fig. 10), which contains the rates between the magnetic substates $A(M'_J \rightarrow M_J)$ as well as the fine structure energies. For ^{47}Ti MITHIT produces the output file `even.odd.hfs.mit.mtrans` (see Fig. 11), which contains the rates between the magnetic substates $A(M'_F \rightarrow M_F)$ and the hyperfine structure energies.

6.6. Test case 6

In the sixth case, the programs are applied to the $4s4d\ ^3D_2$ - $4s4f\ ^3F_{2,3}$ transitions between hyperfine levels in Ga II. Ga II has two stable isotopes with the natural composition of 60% ^{69}Ga and 40% ^{71}Ga, both with nuclear spin $I = 3/2$. The nuclear magnetic moments are, respectively, $\mu_I = 2.01659$ nm and $\mu_I = 2.56227$ nm. The data, e.g. hyperfine interaction matrix elements and transition data, used to produce the spectra in this work are adopted from [39]. The user can find the GRASP2018 scripts for the computation of the fine

structure energies, transition data and reduced hyperfine and Zeeman matrix elements in `examples/test6/script`. Session log for this test run can be found in `examples/test6`.

To compare with the Fourier transform spectra [40], we compute the transition rates between hyperfine levels for ^{69}Ga and ^{71}Ga, respectively. With the calculated hyperfine energies and transition rates between hyperfine levels obtained from MITHIT the synthetic spectra with a Gaussian profile are generated and displayed in Figure 12. Here we employ the experimental fine-structure energies and use the same FWHM values with [39], FWHM = 7.5×10^{-2} cm^{-1} for ^{69}Ga and with a scaling factor 0.986 for ^{71}Ga. Compared with the Fourier transform spectra in Fig. 3 of [40], a good agreement is found.

7. Acknowledgment

PJ and TB acknowledge support from the Swedish Research Council under contract 2015-04842, and JG from the project grant "The New Milky Way" from the Knut and Alice Wallenberg Foundation.

References

[1] P. Indelicato, F. Parente and R. Marrus, Phys. Rev. A 40 (1989) 3505

[2] F. Robicheaux, T. W. Gorczyca, M. S. Pindzola and N. R. Badnell, Phys. Rev. A, 52 (1995) 1319

[3] W. R. Johnson, K. T. Cheng and D. R. Plante Phys. Rev. A 55 (1997) 2728

[4] T. Brage, P. G. Judge, Abdellatif Aboussaïd, M. R. Godefroid and P. Jönsson and A. Ynnerman, C. F. Fischer, D. S. Leckrone, Astrophys. J. 500 (1998) 507.

[5] P. Beiersdorfer, J. H. Scofield, A. L. Osterheld, Phys. Rev. Lett. 90 (2003) 235003.

[6] M. Andersson, J. Grumer, N. Ryde, R. Blackwell-Whitehead, R. Hutton, Y. Zou, P. Jönsson, T. Brage, Astrophys. J. Suppl. S. 216(1) (2014) 2.

[7] J. Grumer, T. Brage, M. Andersson, J. Li, P. Jönsson, W. Li, Y. Yang, R. Hutton, Y. Zou, Phys. Scr. 89 (2014) 114002.

[8] W. Li, J. Grumer, Y. Yang, T. Brage, K. Yao, C. Chen, T. Watanabe,P. Jönsson, H. Lundstedt, R. Hutton, Y. Zou, Astrophys. J. 807 (2015) 69.

[9] W. Li, Y. Yang, B. Tu, J. Xiao, J. Grumer, T. Brage, T. Watanabe, R. Hutton, Y. Zou, Astrophys. J. 826 (2016) 219.

[10] O. Kochukhov, A&A 483 (2008) 557

[11] C.F. Fischer, Comput. Phys. Commun., 64 (1991) 369.

[12] C. F. Fischer, T. Brage, P. Jönsson, Computational Atomic Structure. An MCHF Approach (Institute of Physics Publishing, Bristol/Philadelphia, 1997).

[13] M. F. Gu, Can. J. Phys, 86 (2008) 675.

[14] S. Fritzsche, Comput. Phys. Commun, 240 (2019) 1.

[15] M.G. Kozlov and S.G. Porsev and M.S. Safronova and I.I. Tupitsyn, Comput. Phys. Commun 195 (2015) 199.

[16] P. Jönsson, G. Gaigalas, J. Bieroń, C. F. Fischer, I. P. Grant, Comput. Phys. Commun 184 (2013) 2197.

[17] C. F. Fischer, G. Gaigalas, P. Jönsson, J. Bieroń, Comput. Phys. Commun 237 (2019) 184.

[18] I. P. Grant, Relativistic Quantum Theory of Atoms and Molecules, Springer, New York, 2007.

[19] P Jönsson, G. Gaigalas, P. Rynkun, L. Radžiūtė, J. Ekman, S. Gustafsson, H. Hartman, K. Wang, M. Godefroid, C. F. Fischer, I. Grant, T. Brage, G. Del Zanna, Atoms 5 (2017) 16.

[20] Z. B. Chen, X. L. Guo, K. Wang, J. Quant. Spectrosc. Radiat. Transf. 206 (2018) 213.

[21] M. Andersson, P. Jönsson, Comput. Phys. Commun. 178 (2008) 156.

[22] C. F. Fischer, M. Godefroid, T. Brage, P. Jönsson, G. Gaigalas, J. Phys. B: At. Mol. Opt. Phys. 49 (2016) 182004.

[23] I. Lindgren, A. Rosén, Case Studies in Atomic Physics 4 (1975) 93.

[24] N. J. Stone, IAEA Vienna Report No. INDC(NDS)-0658, 2014.

[25] K. T. Cheng, W. J. Childs, Phys. Rev. A 31 (1985) 2775.

[26] R. D. Cowan, The Theory of Atomic Structure and Spectra, University of California Press, 1981.

[27] B. H. Bransden and C. J. Joachain, Physics of Atoms and Molecules, Longman Inc., New York, 1983.

[28] A. Kramida, Yu. Ralchenko, J. Reader and NIST ASD Team, NIST Atomic Spectra Database (ver. 5.6.1), [Online]. Available: `https://physics.nist.gov/asd` [2019, August 13]. National Institute of Standards and Technology, Gaithersburg, MD.

[29] Q. Wu, G. W. F. Drake, J. Phys. B: At. Mol. Opt. Phys. 40 (2007) 393.

[30] K. R. German, Ph.D. thesis, University of Michigan, 1967 (unpublished, cited by [15]).

[31] E. A. Hinds, J. D. Prestage, F. M. J. Pichanick, Phys. Rev. A 33 (1986) 68.

[32] E. A. Hylleraas, Adv. Quantum Chem. Academic Press, 1 (1964) 1.

[33] G. P. Anisimova, L. A. Volkova, R. I. Semenov, G. A. Tsygankova, I. Y.Chubukov, Opt. Spectrosc. 95 (2003) 865.

[34] A. Adler, Y. Malka, Zeitschrift für Physik 266 (1974) 219.

[35] W. R. Johnson, K. T. Cheng, D. R. Plante, Phys. Rev. A 55 (1997) 2728.

[36] J. Grumer, W. Li, D. Bernhardt, J. Li, S. Schippers, T. Brage, P. Jönsson,R. Hutton, Y. Zou, Phys. Rev. A 88 (2013) 022513.

[37] W. Li, P. Jönsson, T. Brage, R. Hutton, Phys. Rev. A 96 (2017) 052508.

[38] J. Li, J. Grumer, W. Li, M. Andersson, T. Brage, R. Hutton, P. Jönsson,Y. Yang, Y. Zou, Phys. Rev. A 88 (2013) 013416.

[39] M. Andersson, P. Jönsson, H. Sabel, J. Phys. B: At. Mol. Opt. Phys. 39 (2006) 4239.

[40] H. Karlsson, U. Litzén, J. Phys. B: At. Mol. Opt. Phys. 33 (2000) 2929.

Figure 2: Session log for the MITHIT program. Energies of magnetic hyperfine substates of $1s2p\ ^3P_{0,1,2}$ are plotted as functions of the strength of the magnetic field (see Figure 3).

```
>> mithit
Name of the Initial state:
>> 1s2p
Name of the Final state:
>> 1s2p
Are the calculations based on a relativistic CI calculation? (Y/N)
>> y
MIT-fs(0), HIT(1) or MIT-hfs(2):
>> 2
Nuclear spin I:
>> 0.5
Nuclear magnetic dipole moment mu:
>> -2.12749772
Nuclear electric quadrupole moment Q:
>> 0
B-field in Tesla (0) or Gauss (1):
>> 1
Give the upper limit for the B-field:
>> 10000
Energies in a.u. (0), cm-1 (1) or MHz (2) ?
>> 2
Start Computation of Energies and Mixing Coefficients
of the Magnetic Sublevels of Initial States
level    E_hfs (a.u.)   FS-LEV    J      F
-----------------------------------------------
1      -2.133267930    1     2     5/2
2      -2.133267660    2     1     3/2
3      -2.133266873    1     2     3/2
4      -2.123935635    3     1     3/2
5      -2.133266974    2     1     1/2
6      -2.133262704    4     0     1/2
7      -2.123935632    3     1     1/2
Would you like a plot of Zeeman splitting with B field? (Y/N)
>> y
Give an index vector of the levels for which the
zeeman patterns should be plotted
>> [1,2,3,5,6]
Energies and the F-value printed in the plot ? (Y/N)
>> y
More plots ? (Y/N)
>> n
Finished 1s2p

Would you like to compute the transition rates? (Y/N)
>> n
MITHIT finished
```

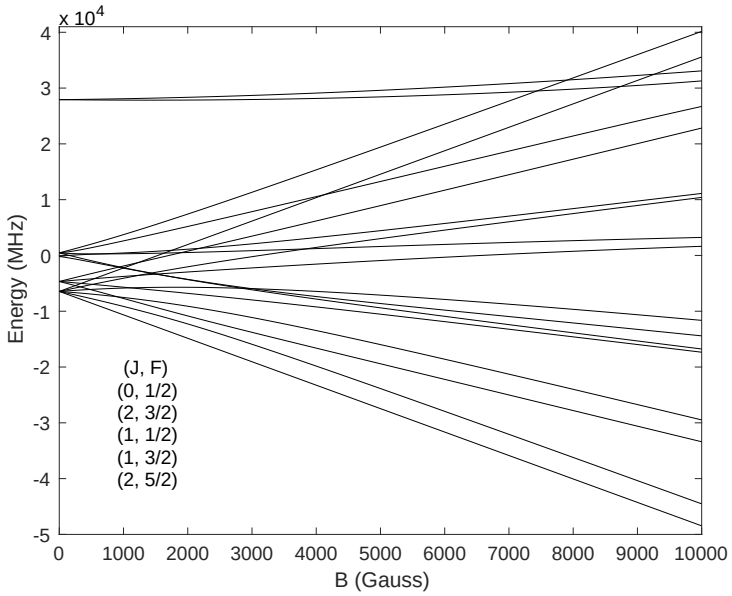

Figure 3: Energies of magnetic hyperfine substates of (^{3}He) $1s2p\ ^3P_{0,1,2}$ as functions of the strength of the magnetic field. The displayed energies are relative to the weighted average energy at zero field. The comparison of the crossings with experimental values is shown in Table 1.

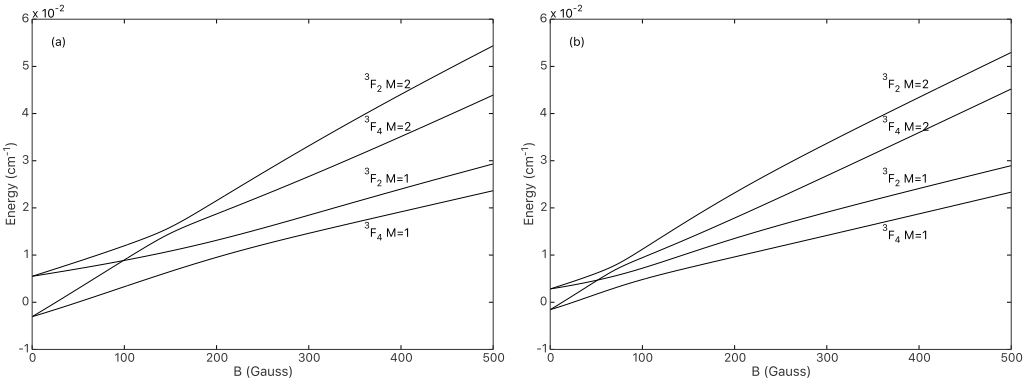

Figure 4: Anticrossings of the magnetic substates of Helium (^{4}He) $1s4f\ ^3F_{2,4}$ (left panel) and $1s5f\ ^3F_{2,4}$ (right panel) as functions of the strength of the magnetic field.

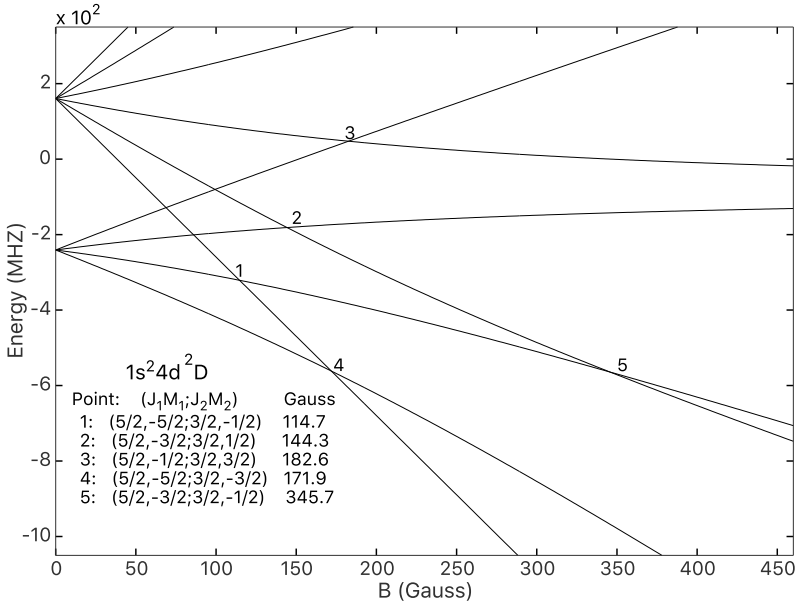

Figure 5: Energies of magnetic substates of lithium (^{6}Li) $1s^2 4d\ ^2D_{5/2,3/2}$ as functions of the strength of the magnetic field. Five crossing points of the substates are marked and the corresponding magnetic field strengths are given in the figure. The comparison with experimental values is shown in Table 2.

Table 1: Comparison between the M_F-dependent substate crossings in ^{3}He $1s2p\ ^3P_{0,1,2}$ obtained with MITHIT and the result of other calculations [29] and experimental values from [30]. The magnetic field strength is given in units of Gauss.

	Crossing substates		B-field (Gauss)		
Point	$(J_1, F_1), M_{F_1})$	(J_2, F_2, M_{F_2})	MITHIT	Ref.[29]	Exp.[30]
1	(1, 1/2, 1/2)	(2, 3/2, -3/2)	160.971	160.8422	160.831
2	(2, 5/2, 5/2)	(1, 3/2, -3/2)	249.095	249.262	
3	(2, 5/2, 3/2)	(1, 3/2, -3/2)	328.158	328.3754	
4	(2, 5/2, 5/2)	(1, 3/2, -1/2)	342.867	343.102	
5	(2, 5/2, 1/2)	(1, 3/2, -3/2)	480.652	480.9610	480.963
6	(2, 5/2, 3/2)	(1, 3/2, -1/2)	517.939	518.2855	518.285
7	(2, 5/2, 5/2)	(1, 3/2, 1/2)	544.386	544.7925	544.793
8	(1, 1/2, 1/2)	(2, 3/2, -1/2)	649.398	647.7145	647.852
9	(2, 5/2, -1/2)	(1, 3/2, -3/2)	900.253	900.728	900.765
10	(1, 3/2, 3/2)	(1, 1/2, -1/2)	925.102	925.3176	925.323
11	(2, 3/2, -3/2)	(1, 3/2, 3/2)	947.508	947.4447	
12	(2, 5/2, 5/2)	(1, 1/2, -1/2)	998.548	998.9944	
13	(2, 5/2, 5/2)	(2, 3/2, -3/2)	1013.294	1013.5076	
14	(2, 5/2, 1/2)	(1, 3/2, -1/2)	1111.375	1111.987	1112.042
15	(2, 5/2, 5/2)	(1, 3/2, 3/2)	1232.279	1233.584	1233.566
16	(2, 5/2, 3/2)	(1, 3/2, 1/2)	1243.352		
17	(2, 5/2, 3/2)	(1, 1/2, -1/2)	1433.456	1434.0633	1434.081
18	(2, 5/2, 3/2)	(2, 3/2, -3/2)	1438.693	1438.823	
19	(1, 3/2, 1/2)	(1, 1/2, -1/2)	1520.361	1520.682	
20	(1, 3/2, 1/2)	(2, 3/2, -3/2)	1524.161	1523.7742	1523.780
21	(1, 1/2, -1/2)	(2, 3/2, -3/2)	1613.769	1595.704	1595.695
22	(2, 5/2, 5/2)	(2, 3/2, -1/2)	1644.447	1644.203	
23	(2, 5/2, 5/2)	(1, 1/2, 1/2)	1763.907	1763.790	1763.803
24	(1, 3/2, 3/2)	(2, 3/2, -1/2)	1908.803	1907.107	
25	(1, 3/2, 3/2)	(1, 1/2, 1/2)	2207.709	2205.307	2205.220
26	(2, 5/2, 1/2)	(2, 3/2, -3/2)	2862.342	2859.490	
27	(2, 5/2, 1/2)	(1, 1/2, -1/2)	3003.239	3001.283	3001.414
28	(2, 5/2, 3/2)	(2, 3/2, -1/2)	3847.903	3841.227	
29	(2, 5/2, 5/2)	(2, 3/2, 1/2)	4143.483	4137.720	4137.743
30	(2, 3/2, 3/2)	(0, 1/2, 1/2)	7430.707	7436.796	
31	(2, 3/2, 3/2)	(0, 1/2, -1/2)	7903.939	7903.917	7903.978
32	(2, 5/2, 5/2)	(0, 1/2, 1/2)	8747.245	8747.236	8747.303
33	(2, 5/2, 5/2)	(0, 1/2, -1/2)	9270.119	9262.1496	

	Crossing substates		B-field (Gauss)	
Point	$^2D_{5/2}(M_J)$	$^2D_{3/2}(M_J)$	MITHIT	Exp.[34]
1	-5/2	-1/2	114.7	112(3)
2	-3/2	1/2	144.3	147(15)
3	-1/2	3/2	182.6	183(10)
4	-5/2	-3/2	171.9	169(3)

Table 2: Comparison between the M_J-dependent substate crossings in ^{6}Li $1s^2 4d\ ^2D_{5/2,3/2}$ obtained with MITHIT and experimental values from [34]. The magnetic field strength is given in units of Gauss.

Table 3: Hyperfine-induced transition rates $A(1s2p\ ^3P_0\ F' = I \rightarrow\ 1s^2\ ^1S_0\ F = I)$ in He-like ions ($6 \leq Z \leq 30$). The rates are compared with results from Ref. [35]. All transition rates are given in s^{-1} and x[n] represent x·10^n.

Ions	Z	I	μ_I	A	Ref. [35]
^{13}C	6	1/2	0.70241	1.133[5]	1.1[5]
^{15}N	7	1/2	-0.28319	5.205[5]	5.4[5]
^{17}O	8	5/2	-1.8938	2.575[6]	2.6[6]
^{19}F	9	1/2	2.6289	1.427[7]	1.391[7]
^{21}Ne	10	3/2	-0.6618	6.398[5]	6.0[5]
^{23}Na	11	3/2	2.2176	1.193[7]	1.19[7]
^{25}Mg	12	5/2	-0.85545	2.413[6]	2.4[6]
^{27}Al	13	5/2	3.6415	7.376[7]	7.37[7]
^{29}Si	14	1/2	-0.55529	5.900[6]	5.9[6]
^{31}P	15	1/2	1.1316	4.092[7]	4.09[7]
^{33}S	16	3/2	0.64382	1.158[7]	1.16[7]
^{35}Cl	17	3/2	0.82187	2.976[7]	2.97[7]
^{37}Cl	17	3/2	0.68412	2.061[7]	2.06[7]
^{39}K	19	3/2	0.39149	1.606[7]	1.6[7]
^{41}K	19	3/2	0.21488	4.834[6]	4.8[6]
^{41}Ca	20	7/2	-1.5948	3.099[8]	3.095[8]
^{43}Ca	20	7/2	-1.3176	2.116[8]	2.114[8]
^{45}Sc	21	7/2	4.7565	4.184[9]	4.181[9]
^{47}Ti	22	5/2	-0.78848	1.838[8]	1.836[8]
^{49}Ti	22	7/2	-1.1042	3.310[8]	3.307[8]
^{51}V	23	7/2	5.1487	1.073[10]	1.073[10]
^{53}Cr	24	3/2	-0.47454	1.706[8]	1.705[8]
^{51}Mn	25	5/2	3.5683	1.193[10]	1.193[10]
^{55}Mn	25	5/2	3.4687	1.127[10]	1.127[10]
^{57}Fe	26	1/2	0.09062	2.361[7]	2.36[7]
^{59}Co	27	7/2	4.627	3.832[10]	3.832[10]
^{61}Ni	28	3/2	-0.75002	1.844[9]	1.845[9]
^{63}Cu	29	3/2	2.2273	2.380[10]	2.38[10]
^{65}Cu	29	3/2	2.3816	2.724[10]	2.724[10]
^{67}Zn	30	5/2	0.8752	4.374[9]	4.373[9]

Figure 6: Session log for the MITHIT program for the computation of hyperfine-induced transitions rates $A(1s2p\ ^3P_0\ F' = I \rightarrow\ 1s^2\ ^1S_0\ F = I)$ for He-like ^{19}F.

```
>> mithit
Name of the Initial state:
>> even
Name of the Final state:
>> odd
Are the calculations based on a relativistic CI calculation? (Y/N)
>> y
MIT-fs(0), HIT(1) or MIT-hfs(2):
>> 1
Nuclear spin I:
>> 0.5
Nuclear magnetic dipole moment mu:
>> 2.6289
Nuclear electric quadrupole moment Q:
>> 0
Start Computation of Energies and Mixing Coefficients
of the Magnetic Sublevels of Initial States
level E_hfs (a.u.) FS-LEV J F
-----------------------------------------------
1 -49.031526398 1 1 3/2
2 -75.595184342 2 0 1/2
3 -49.031649658 1 1 1/2
4 -48.698681617 3 0 1/2
Finished even

Start Computation of Energies and Mixing Coefficients
of the Magnetic Sublevels of Final States

level E_hfs (a.u.) FS-LEV J F
-----------------------------------------------
1 -48.705022799 1 2 5/2
2 -48.709369042 2 1 3/2
3 -48.705116687 1 2 3/2
4 -48.485445256 3 1 3/2
5 -48.710076484 4 0 1/2
6 -48.709425705 2 1 1/2
7 -48.485444841 3 1 1/2
Finished odd
```

```
Would you like to compute the transition rates? (Y/N)
>> y

level E_hfs (a.u.) FS-LEV J F
------------------------------------------------------------
Initial levels:
1 -49.031526398 1 1 3/2
2 -49.031649658 1 1 1/2
3 -75.595184342 2 0 1/2
4 -48.698681617 3 0 1/2
Final levels:
1 -48.705022799 1 2 5/2
2 -48.705116687 1 2 3/2
3 -48.709369042 2 1 3/2
4 -48.709425705 2 1 1/2
5 -48.485445256 3 1 3/2
6 -48.485444841 3 1 1/2
7 -48.710076484 4 0 1/2
Give an index vector of the initial levels(lower level):
>> 3
Give an index vector of the final levels(upper level):
>> 7
Would you like a plot of synthetic spectra? (Y/N)
>> n
MITHIT finished
```

Figure 7: The MITHIT output file `even.odd.hfs.hit.trans` containing the transition rates $A(1s2p\ ^3P_0\ F' = I \rightarrow 1s^2\ ^1S_0\ F = I)$ for He-like ^{19}F.

```
Nuclear data
Nuclear spin                          0.500000 au
Nuclear magnetic dipole moment        2.628900 n.m.
Nuclear electric quadrupole moment    0.000000 barns

Hyperfine structure energies in a.u.
even
level J F E_hfs (a.u.) FS-LEV
1  1.0  1.5 -49.031526 1
2  1.0  0.5 -49.031650 1
3  0.0  0.5 -75.595184 2
4  0.0  0.5 -48.698682 3
odd
level J F E_hfs (a.u.) FS-LEV
1  2.0  2.5 -48.705023 1
2  2.0  1.5 -48.705117 1
3  1.0  1.5 -48.709369 2
4  1.0  0.5 -48.709426 2
5  1.0  1.5 -48.485445 3
6  1.0  0.5 -48.485445 3
7  0.0  0.5 -48.710076 4

Transition rates and wavelength in Kays
Upper                                          Lower
level J   F     E_hfs (a.u.) FS-LEV level  J   F   E_hfs (a.u.) FS-LEV  A (s-1)       E (Kays)
 7  0.0 0.5  -48.710076484    4  3  0.0  0.5  -75.595184342  2   1.4274E+07  5900599.117926516
```

Figure 8: Session log for the MITHIT program for the computation of magnetic-field-induced transitions $A(2s2p\ ^3P_0\ M'_J \rightarrow 2s^2\ ^1S_0\ M_J)$ for Be-like ^{48}Ti with zero nuclear spin.

```
>> mithit
Name of the Initial state:
>> even.22
Name of the Final state:
>> odd.22
Are the calculations based on a relativistic CI calculation? (Y/N)
>> y
MIT-fs(0), HIT(1) or MIT-hfs(2):
>> 0
B-field in Tesla (0) or Gauss (1):
>> 0
Give the upper limit for the B-field:
>> 1
Energies in a.u. (0), cm-1 (1) or MHz (2) ?
>> 1
Start Computation of Energies and Mixing Coefficients
of the Magnetic Sublevels of Initial States
level E_fs (a.u.) J
-----------------------------------------------
1 -575.022701901 0
 Would you like a plot of Zeeman splitting with B field? (Y/N)
>> n
Finished even.22

Start Computation of Energies and Mixing Coefficients
of the Magnetic Sublevels of Final States
level E_fs (a.u.) J
-----------------------------------------------
1 -573.440650516 2
2 -573.635009436 1
3 -572.334288837 1
4 -573.709983113 0
 Would you like a plot of Zeeman splitting with B field? (Y/N)
>> n
Finished odd.22

Would you like to compute the transition rates? (Y/N)
```

```
>> y
level E_BP (a.u.) J
-------------------------------
Initial levels:
1 -575.022701901 0
Final levels:
1 -573.440650516 2
2 -573.635009436 1
3 -572.334288837 1
4 -573.709983113 0
Give an index vector of the initial levels(lower level):
>> 1
Give an index vector of the final levels(upper level):
>> 4
Would you like a plot of synthetic spectra? (Y/N)
>> n
MITHIT finished
```

Figure 9: Session log for the MITHIT program for the computation of magnetic-field-induced transitions $A(2s2p\ ^3P_0\ M'_F \rightarrow 2s^2\ ^1S_0\ M_F)$ of the hyperfine substates for Be-like ^{47}Ti.

```
>> mithit
 Name of the Initial state:
>> even.22
 Name of the Final state:
>> odd.22
 Are the calculations based on a relativistic CI calculation? (Y/N)
>> y
 MIT-fs(0), HIT(1) or MIT-hfs(2):
>> 2
 Nuclear spin I:
>> 2.5
 Nuclear magnetic dipole moment mu:
>> -0.78848
 Nuclear electric quadrupole moment Q:
>> 0.302
 B-field in Tesla (0) or Gauss (1):
>> 0
 Give the upper limit for the B-field:
>> 1
 Energies in a.u. (0), cm-1 (1) or MHz (2) ?
>> 1
 Start Computation of Energies and Mixing Coefficients
 of the Magnetic Sublevels of Initial States
 level E_hfs (a.u.) FS-LEV J F
 ------------------------------------------------
 1 -575.022701900 1 0 5/2
  Would you like a plot of Zeeman splitting with B field? (Y/N)
>> n
 Finished even2s2

 Start Computation of Energies and Mixing Coefficients
 of the Magnetic Sublevels of Final States
 level E_hfs (a.u.) FS-LEV J F
 ------------------------------------------------
  1 -573.440671634 1 2 9/2

  ......
```

```
 12 -573.440620455 1 2 1/2
  Would you like a plot of Zeeman splitting with B field? (Y/N)
>> n
 Finished odd2s2p

 Would you like to compute the transition rates? (Y/N)
>> y
 level E_hfs (a.u.) FS-LEV J F
 ------------------------------------------------------------
 Initial levels:
 1 -575.022701900 1 0 5/2
 Final levels:
  1 -573.440671634 1 2 9/2

  ......

 12 -573.709983115 4 0 5/2
 Give an index vector of the initial levels(lower level):
>> 1
 Give an index vector of the final levels(upper level):
>> 12
 Would you like a plot of synthetic spectra? (Y/N)
>> n
 MITHIT finished
```

Figure 10: The MITHIT output file `even2s2.odd2s2p.fs.mit.mtrans` containing the fine structure energies and transition rates $A(2s2p\ ^3P_0\ M'_J \rightarrow 2s^2\ ^1S_0\ M_J)$ for Be-like ^{48}Ti.

```
Magnetic field
B  =       1.0000000 Tesla

Fine structure energies in a.u.
even.22
level J E_BP (a.u.)
1  0.0 -575.022702

odd.22
level J E_BP (a.u.)
1  2.0 -573.440651
2  1.0 -573.635009
3  1.0 -572.334289
4  0.0 -573.709983

Transition rates and wavelength in Kays
Upper Lower
level J  M_J    E_hfs (a.u.)  FS-LEV  level  J  M_J  E_hfs (a.u.)  FS-LEV  A (s-1)   E (Kays)
 4  0.0 0.0   -573.709983113  4  1 0.0 0.0   -575.022701901   1 5.6887E-03  288108.471182994
```

Figure 11: The MITHIT output file `even2s2.odd2s2p.hfs.mit.mtrans` containing the hyperfine structure energies and transition rates $A(2s2p\ ^3P_0\ M'_F \rightarrow 2s^2\ ^1S_0\ M_F)$ for Be-like ^{47}Ti.

```
B                                    1.000000 T
Nuclear spin                         2.500000 au
Nuclear magnetic dipole moment      -0.788480 n.m.
Nuclear electric quadrupole moment   0.302000 barns

level     J     F     E_hfs (a.u.)     FS-LEV
even.22
 1      0.0      2.5     -575.022702          1
odd.22
 1      2.0      4.5     -573.440672          1
 2      2.0      3.5     -573.440653          1
 3      2.0      2.5     -573.440638          1
 4      2.0      1.5     -573.440627          1
 5      2.0      0.5     -573.440620          1
 6      1.0      3.5     -573.635025          2
 7      1.0      2.5     -573.635003          2
 8      1.0      1.5     -573.634987          2
 9      1.0      3.5     -572.334290          3
10      1.0      2.5     -572.334289          3
11      1.0      1.5     -572.334287          3
12      0.0      2.5     -573.709983          4

           Upper                                          Lower
level  J  F  M_F     E_hfs (a.u.) FS-LEV level  J  F  M_F  E_hfs (a.u.) FS-LEV  A (s-1)    E (Kays)
12 0.0 2.5 2.5   -573.709983115  4  1 0.0 2.5  2.5   -575.022701901  1 3.8149E-01 288108.470744049
12 0.0 2.5 2.5   -573.709983115  4  1 0.0 2.5  1.5   -575.022701901  1 1.9214E-01 288108.470744049
12 0.0 2.5 2.5   -573.709983115  4  1 0.0 2.5  0.5   -575.022701901  1 2.2531E-13 288108.470744049
12 0.0 2.5 2.5   -573.709983115  4  1 0.0 2.5 -0.5   -575.022701901  1 0.0000E+00 288108.470744049
12 0.0 2.5 2.5   -573.709983115  4  1 0.0 2.5 -1.5   -575.022701901  1 0.0000E+00 288108.470744049
12 0.0 2.5 2.5   -573.709983115  4  1 0.0 2.5 -2.5   -575.022701901  1 0.0000E+00 288108.470744049

  ......

12 0.0 2.5 -2.5   -573.709983116  4  1 0.0 2.5  2.5   -575.022701901  1 0.0000E+00 288108.470524577
12 0.0 2.5 -2.5   -573.709983116  4  1 0.0 2.5  1.5   -575.022701901  1 0.0000E+00 288108.470524577
12 0.0 2.5 -2.5   -573.709983116  4  1 0.0 2.5  0.5   -575.022701901  1 0.0000E+00 288108.470524577
12 0.0 2.5 -2.5   -573.709983116  4  1 0.0 2.5 -0.5   -575.022701901  1 2.2536E-13 288108.470524577
12 0.0 2.5 -2.5   -573.709983116  4  1 0.0 2.5 -1.5   -575.022701901  1 1.9213E-01 288108.470524577
12 0.0 2.5 -2.5   -573.709983116  4  1 0.0 2.5 -2.5   -575.022701901  1 5.9058E-01 288108.470524577
```

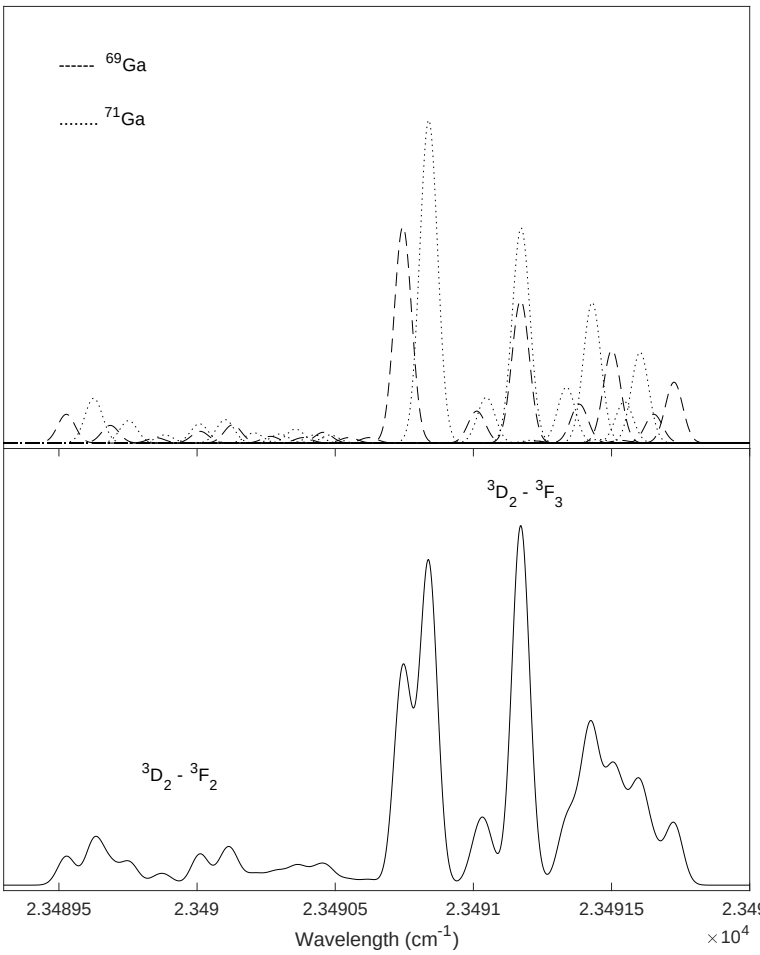

Figure 12: Synthetic spectrum of Ga II for the transitions between $4s4d\ ^3D_2$ and $4s4f\ ^3F_{2,3}$. The figure in the upper panel displays the spectra of the individual hyperfine components in the synthetic spectrum. Dashed and dotted lines show, respectively, the contributions from ^{69}Ga and ^{71}Ga. The intensity of the hyperfine components within each isotope are weighted in accordance to the relative abundance of the two isotopes, 60% ^{69}Ga and 40% ^{71}Ga.